CHARACTERIZATION OF Nd:YAG PULSED LASER WELDED AUSTENITIC AISI 304 STAINLESS STEEL

CODIGO DO TRABALHO: 021018171

Abstract: Over the last two decades, laser beam welding has became established as an economically sound and high quality joining process ideal for many industrial applications. . Welding with laser technology offers a number of advantages over conventional welding methods. It improves efficiency, simplifies handling, provides high quality, and laser-welded parts require less refinishing. These advantages are a result of focused energy input,narrow heat-affect zone, and minimal distortion of the work-piece. One problem of importance is to control the critical gap employed in butt-joint thin sheet design that should be considered, especially if the application is to be repeated in high-volume production. Butt joints are sensitive to gaps and the gap tolerance is dependent on material thickness, weld speed, beam diameter, and beam quality. Normally, gap tolerance increases with material thickness. However, as the gap increases, the reinforcement of laser welds decreases. As the gap continues to increase, underfill will became more severe until complete lack of fusion occurs. Experimental investigations were carried out using a pulsed neodymium: yttrium aluminium garnet (Nd:YAG) laser welding *to examine the influence of the joint gap in the characteristics of austenitic stainless steel AISI 304 weld fillet, such as weld metal geometry, heat-affected-zone extension, microhardness profile, content of δ-ferrite, presence of spatters, discontinuities such as vapor pores, weld metal microcracks, root and crater cracks.*

Keywords: welding, pulsed Nd:YAG laser, joint gap,austenitic stainless steel, AISI 304.

1. INTRODUCTION

Laser beam welding is used to join austenitic stainless steels featuring precise control, high welding speeds when joining thin sections, and welds with high depth-to-width ratios in thick sections. The heat-affected zone in this weld is usually much narrower than those of welds made by the conventional welding processes and is not likely to be sensitized to corrosion. Welding with pulsed Nd:YAG Laser System is characterized by periodic heating of the weld pool by a high peak power density pulsed laser beam incident that allow melting and solidification to take place consecutively. However, due to very high peak power density involved in pulsed laser welding, the solidification time is orders of magnitude shorter than conventional welds. Combination of process parameters such as pulse energy $[E_p]$, pulse duration $[t_p]$, pulse frequency $[f_p]$ and welding speed $[v]$ determines the welding mode, that is, conduction or keyhole.

Alloy selection for pulsed YAG laser beam welding, or other processes producing rapid solidification rates, becomes much more restrictive and critical, to ensure resistance to cracking. Stainless steel of the 300 series, with the exception of free machining Types 303 and 303Se and stabilized Types 321 and 347 are good candidates for laser welding. AISI 304 stainless steels have many advantages such as low thermal conductivity, high resistance to corrosion and high stability at elevated temperatures and also it is a superior absorber of laser light. Due to these advantages, it is used in numerous industries including electronics, chemical, nuclear, medical instruments, home appliances, automotive and specialized tube industry (AWS, 1998).

Porosity is detrimental to welds quality. It has been frequently observed in deep penetration pulsed laser welds. Its formation is associated with weld pool dynamics and keyhole collapse. Porosity will be formed in pulsed laser welding if the solidification rate of the molten metal exceeds the backfilling speed of liquid metal during keyhole collapse. (Zhou et al., 2007).

A gap is one of the most important issues to be solved in laser welding of butt joint, because the gap results in welding defects such as underfilling or a non-bonded joint. Butt joints are sensitive to gaps. The gap tolerance for butt-

joints is dependent on material thickness, weld speed, beam diameter, and beam quality. Normally, gap tolerance increases with material thickness. However, as the gap increases, the reinforcement normally associated with line-on-line fit up of laser welds decreases. When the gap is too large for weld bead reinforcement, underfill will occur. As the gap continues to increase, underfill will become more severe until complete lack of fusion occurs. This condition is characterized by the beam actually channeling through the gap without being absorbed by the workpiece at the melting surface. The gap tolerance has a relatively narrow band which is related to work piece thickness and beam spot size, however the minimum gap specified should be based on the factors mentioned above as well as the required fusion zone geometry (AWS, 1991).

The effect of joint gap on the strength of partial penetration butt welds was stated by Wouters et al. (2006). The results showed that a zero gap gave a weak weld because the weld geometry contained the equivalent of a sharp crack where the unweld parts met each other. A small gap between the workpieces improved the weld impact strength as the sharp crack effect became dissipated. Further increases in gap width resulted in a weakening of the joint because decreases the molten metal area.

There are some reports (Kawarito et al., 2007 and Deng et al., 2004) which deal with the shape and characteristics of the fusion zone in relation to different gaps for laser welding. However, this issue has up to now not been extensively researched. More work is required for understanding the effect of the gap on the shape and microstructure of the fusion zone.

The present investigation is concerned with joint gap on pulsed neodymium: yttrium aluminium garnet (Nd:YAG) laser welding of austenitic stainless steel AISI 304 and its effect on fusion zone characteristics.

2. EXPERIMENTAL PROCEDURE

The research work was planned to be carried out with a pulsed Nd:YAG Laser Welding System. The experimental set up adopted is shown in Fig. 1.

The base material used for this study was the AISI 304 stainless steel with 0.8 mm thickness. It was cut to size of 20mm x 50mm. The chemical composition is shown in table 1. The parameters used in this experiment are given in table 2. The experimental results were analyzed on the basis of the relationships between gaps and weld bead shape and dimensions. The specimens were prepared and cleaned to assure that all samples presented the same surface conditions with a homogeneous finish.
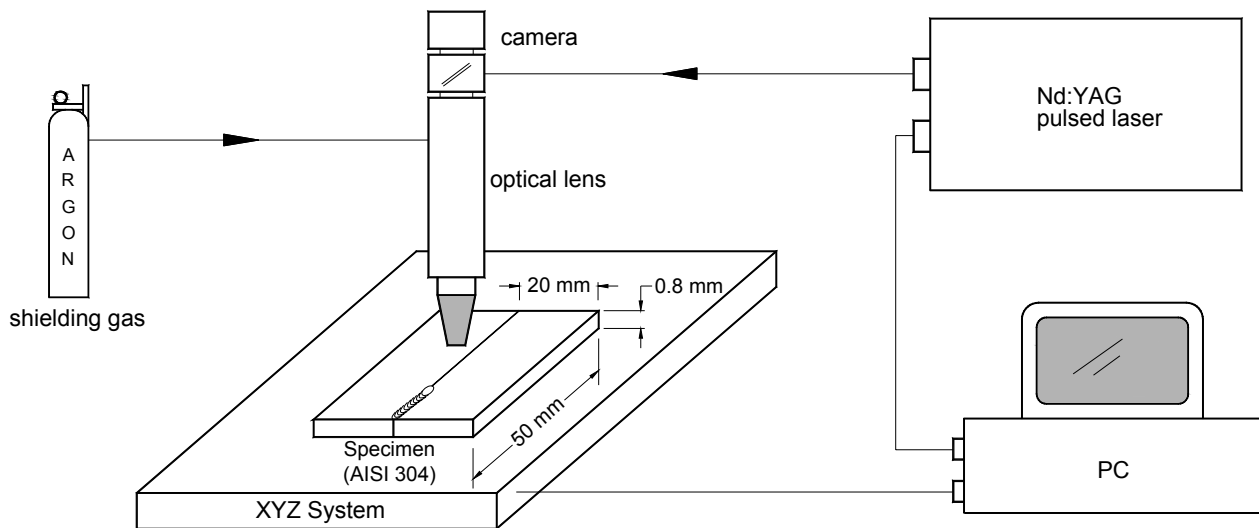

Figure 1. Schematic diagram of laser welding system.

**Table 1. Typical chemical analysis of the base metal used (wt %).**

	C	Mn	Si	P	S	Cr	Ni	Mo	Co	Cu	N
AISI304	0.037	1.24	0.53	0.034	0.002	18.09	8.07	0.12	0.115	0.188	0.0476

Table 2. Pulsed Nd:YAG laser welding parameters.

Parameter	Symbol	Unit	Level
Beam diameter	Φ_b	mm	0.2
Beam angle	A_b	degree	90
Pulse energy	E_p	J	5.3
Pulse frequency	f_p	H_Z	10
Pulse duration	t_p	ms	7
Average power	P_m	W	53
Welding speed	v	mm/min	150
Flow rate	F_r	l/min	10

To evaluate the influence of the gap, welding was carried out using 02 pairs of specimens positioned as butt joints. The first was positioned with zero gap (Fig. 2a). The second was positioned with variable root opening in order to afford different gaps (Fig. 2b). All others processing parameters were kept constant. The specimens were held firmly using fixture to prevent distortion and then laser-welded in an argon atmosphere at a flow rate of 10 l/min. None of the specimens was subjected to any subsequent form of heat treatment or machining.

After welding, specimen with zero gap was cut from transverse sections at the mid-length position of the weld. The other, was cut in different positions, resulting in gaps 60, 160, 235, 280 and 330 µm. Finally, the cut surfaces were prepared for metallographic inspection by polishing and etching to display bead shape and microstructure. The bead shape measurements were made using an optical microscope with an image analysis system.
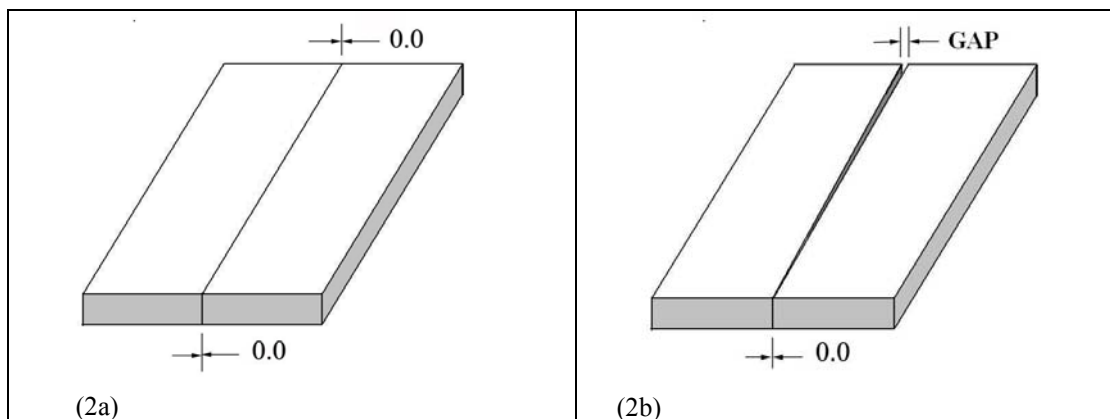
Figure 2. Butt joints with zero gap (2a) and variable gap (2b).

Microhardness (HV20) tests were performed on a transverse section of the weld bead (Fig. 3), along the direction parallel to the surface of the sheet, in the centre of the bead, in order to identify the possible effects of microstructural heterogeneities both in the bead, and in the parent metal. The data reported are the average of three individual results.
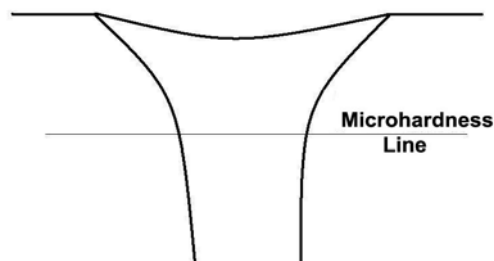
Figure 3. Scheme of the microhardness test position.

3.   RESULTS

The effect of the joint gap was clarified using type 304 steel and pulsed laser of Nd:YAG. Figure 4a shows a top view of welded bead with variable gap. Figures 4b and 4c show details along of the weld bead. It is clearly noticeable in the region of the bead with narrow gap (Fig. 4b) the absence of any detectable defect on surface of the bead and adjacencies. Figure 4c shows the region with wide gap and where underfill, lack of fusion and high amount of spatter at the top occurred.

3.1 Macrostructure

The weld beads showed characteristic of pulsed laser welding. No welding cracks were found in any of the welds, this may be partly due to the good crack resistance of base metal and the welding conditions provided. Some pores were observed in specimen with zero gap.

The cross section macrostructures of the butt laser welds, as a function of gap size, are summarized in Fig. 5. In Fig. 5a (specimen with zero gap) no depression, at the top and bottom, was observed and the vertical matching appears good; this contributes to the symmetry of the bead. Due to the small thickness of the sheet and to the position of the focus of the beam, depth-to-width ratio of the fusion zone is small (with reference to figure 5a the depth-to-width ratio is 0.72). A slight depression at the top of the bead is noticeable in Fig. 5b, probably due to insufficient matching of the two facing edges. Increasing the gap on the others specimens, Fig. 5c and 5d, an increase occurred with the depression at the top and bottom of the bead, until a complete lack of fusion occurs. The concavity increased proportionality to the gap size. The maximum depth of the concavity, at the top and at the bottom, reached 0.28 and 0.25mm, respectively. Figure 6 shows the effect of the gap on depression at the top and bottom of type 304 steel welds.

The macrostructures indicated also that the weld pool morphology is essentially symmetrical about the axis of the laser beam. This symmetry at the top and bottom side was observed in all joints, independent of the gap, suggesting a steady fluid flow in the weld pool, however, the higher the gap a high amount of spatter at the top occurred. It suggests the presence of strong electromagnetic forces higher than the surface tension gradient forces in the weld pool. This perturbation in the weld pool, with high gap, can change dramatically the flow field, resulting in the observed spatter and lack of fusion, as summarized in Fig. 4c.

The relationship between gap sizes and bead width of 304 steel is summarized in Fig. 7. The bead width decreased from 1.17 to 0.76 mm on changing the joint gap from zero to 330 µm. This indicated that when the laser beam interacts with the specimen, a hole is drilled through the thickness of the material and the cavity is filled with plasma and surrounded by molten metal. This bead width variation is a result of the higher the gap a low amount of material is molten at joint region. In presence of the gap, part of the laser beam passed through the joint before the bridged molten pool was formed and this reduces the process efficiency and so the heat input. The molten metal volume decreases as the joint gap increases, and this contributes to low conductive heat transfer decreasing the bead width. It was founded that the molten pool bridges the gap up to 380 µm.

It noted that the area under laser beam decreases as the joint gap increases at the same laser beam diameter (Φ_b). It has a negative effect associated to a highly focused welding heat source, such as laser beam. The weld spot volume and the portion of the keyhole surface exposed directly to the laser beam are sensitive to the variation of the gap, both decrease with the gap increased as summarized by Kawarito et al.(2007).

The specimen with zero gap showed the presence of pores at the interface between fusion zone and base metal. In presence of wider gaps, no pore was observed. This suggests that a gap between the workpieces improves the fluid flow reducing the presence of pores. On the other hand, the molten metal volume decreased and deeply concave underfills occurred. Figure 8 shows a typical pore at the interface between fusion zone and base metal in the case of zero gap.

These macrostructural results indicated that weld metal characteristics are sensitive to the variation of the gap. In order to obtain an acceptable weld profile, zero or narrow gap between the workpieces are desirable, even though the presence of pores were found in some of the welds. It also be noted that the higher the joint gap, the higher the concavity at the top and bottom of the weld, consequently, a weakening of the weld joint. Moreover, it would be expect that underfills would be suppressed by using a high peak power until the molten pool bridge the gap. Lack of fusion was obtained at joint gap equal to or greater than 380 µm. No welding cracks were observed in any of the welds, suggesting that welding cracks are not sensitive to the variation of the gap; they are function of the Cr_{eq}/Ni_{eq} ratio. Presences of spatters were found in wider gaps.

The most acceptable weld bead was obtained at joint gap of 60 µm, where the molten pool bridged the gap and the weld bead profile showed minimum top and bottom concavity, and no porosity or cracking were observed.
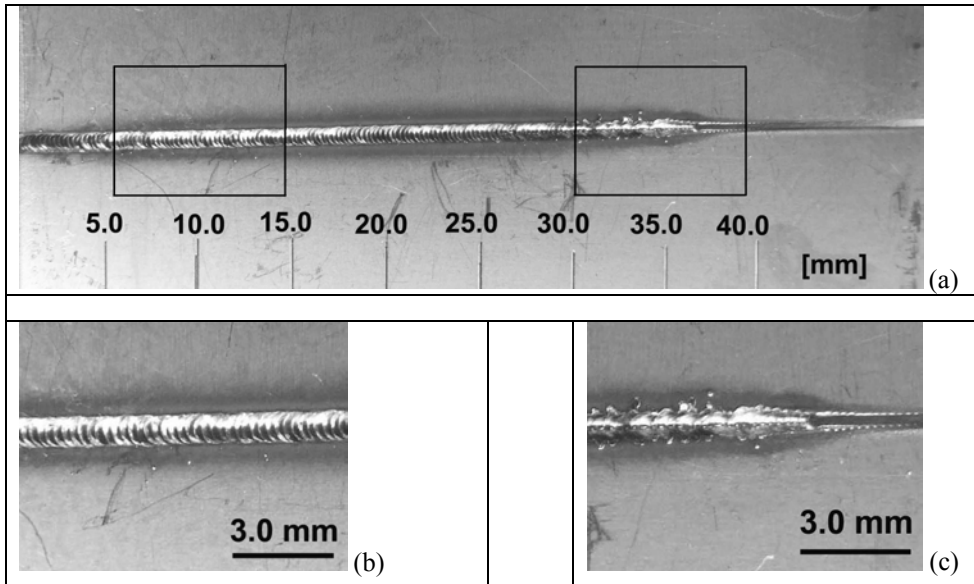
Figure 4. (a)Surface appearance along the weld bead made with Nd:YAG pulsed laser under variable gap condition, (b) narrow gap region, and (c) wide gap region.
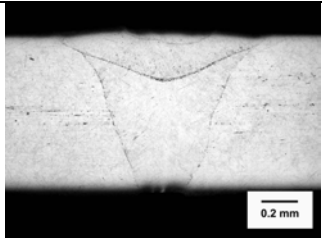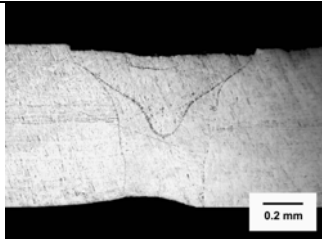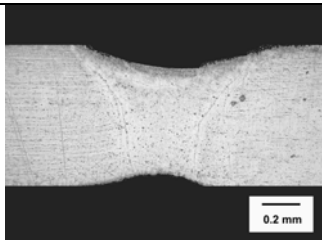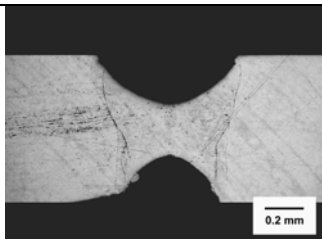

Figure 5. Cross sections of butt joints made with pulsed Nd:YAG laser welding under different gaps. (BW=bead width; SD=surface depression; RD=root depression)
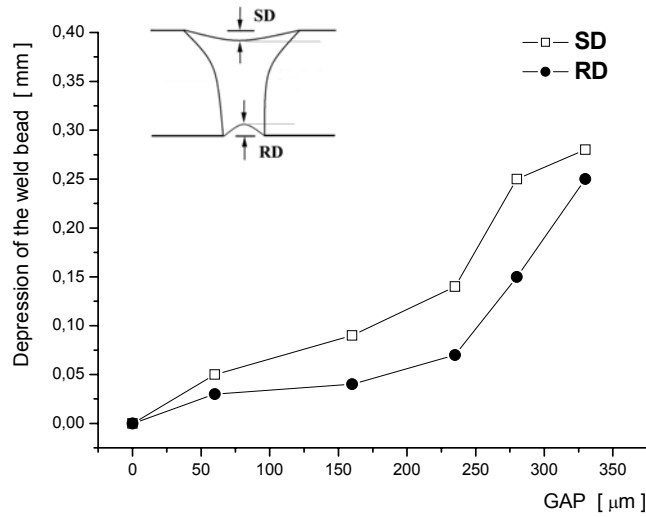
Figure 6. Effect of the gap on depression at the top (SD) and bottom (RD) of the bead.
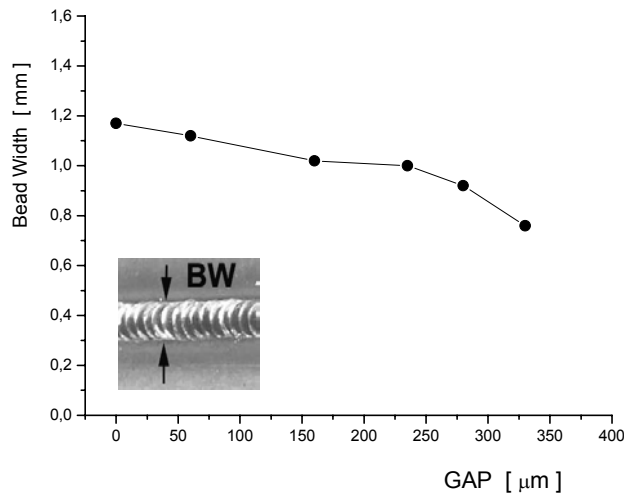

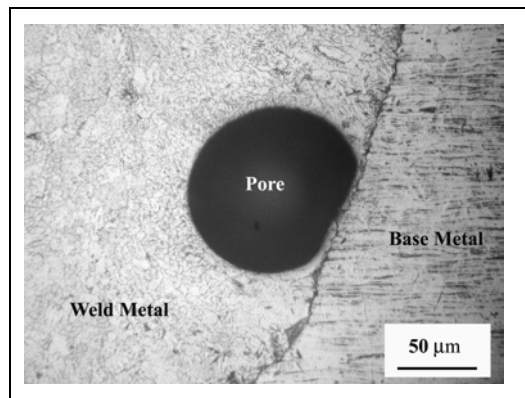**Figure 7. Relationship between gap sizes and bead width.**

Figure 8. Presence of pore at the interface between fusion zone and base metal. Specimen with zero gap.

3.2 Microstructure

The first observation is that the extension of the heat affected zone (HAZ) is negligible. This is valid in all specimens, and is the typical positive effect associated to a highly focused welding heat source, such as laser beam, producing extremely high cooling rates compared to that of conventional GTA welding (Vitek et al., 1983). In these joints the HAZ are not likely to be sensitized to corrosion. It was also found a highly directional nature of the microstructures around the axis of the laser beam due to solidification of the weld metal at high cooling rate.

In the weld bead, a fully dendritic microstructure was detected, in all specimens, with developed primary and distinguishable short secondary arms of delta ferrite (δ). The degree of this transformation (ferrite/austenite) is dependent primarily on the weld metal composition and secondarily on the cooling rate. A vermicular δ ferrite microstructure was observed in all specimens, suggesting a diffusion-controlled, solid-state transformation of ferrite to austenite, following solidification as primary ferrite (mode FA). This morphological form is the most commonly observed in austenitic stainless steel weld metal. Some lathy δ ferrite microstructure was observed in specimens with the highest gaps, around the fusion line, suggesting that ferrite results also from primary ferrite solidification (Type AF) but is characteristically in form of laths that span the solidification subgrain. This ferrite morphology is typical in welds that have been rapidly cooled.

From image analysis determination, it has been seen that the effect of the joint gap in the weld microstructure produced no changes. The dendritic (darker phase) represents 10 to 15% of the bead area, in all specimens, and the interdendritic (lighter phase) the remaining.

From the composition given in Table 1 and from the following formulae (Delong, 1974):

$$Cr_{eq} = \%Cr + \%Mo + 1.5\ \%Si + 0.5\ \%Nb$$

$$Ni_{eq} = \%Ni + 30\ \%C + 0.5\ \%Mn + 30\%N$$

It can be calculated that the steel under investigation has a Cr_{eq} to Ni_{eq} ratio equal to 1.69. This means, using a pseudo binary diagram for prediction of equilibrium microstructure in stainless steel, that the solidification, under equilibrium conditions (but also in presence of high cooling rates), takes place in a ferrite-austenite solidification condition-mode FA(Lippold,1994 and Vitek et al.,1983).

The Suutala diagram has been used successfully for predicting weld solidification behavior and cracking susceptibility in welds made using conventional arc welding processes, however pulsed Nd:YAG laser welding produces extremely rapid solidification and cooling rates, and in this case the Suutala diagram has been found not to be predictive of cracking susceptibility. Using a modified Suutala diagram, proposed by Lippold (1994), for pulsed YAG laser beam welding of austenitic stainless steels and Cr_{eq} / Ni_{eq} ratio, solidification occurred as primary ferrite rather than primary austenite as predicted by conventional diagrams. In addition, this diagram shows a region with no cracking susceptibility. As the result obtained exhibited a Cr_{eq} / Ni_{eq} ratio greater than 1.7, it is consistent with the modified Suutala diagram for predicting microstructure and cracking encountered during pulsed Nd:YAG laser welding of austenitic stainless steel AISI 304. Consequently, it can be deduced that all welds concerned in this investigation were solidified as ferrite-austenite mode and they are not susceptible to cracking.

3.3 Mechanical Properties

Hardness profiles of the base metal, heat affected zone and weld metal of austenitic stainless steel AISI 304 as a function of root opening are shown in Fig. 9. No significant difference between hardness of weld metal and heat affected zone was obtained; hardness of heat affected zone was slightly higher than that of weld metal regardless of gap. Base metal hardness was always lower than that of HAZ and weld metal. These results were valid for all joints. This is expected because mechanical properties of steel, in general, are based on its microstructures.

As can be seen in Fig. 9, the microhardness values (HV20) increased from joints with no gap to maximum gap (330 µm). During the solidification of the fusion zone, the material generally loses its original strength induced by strain hardening. Microhardness profiles in welded joints obtained with higher gaps show an increment of the hardness in the fusion zone and a finer microstructure induced by rapid cooling.
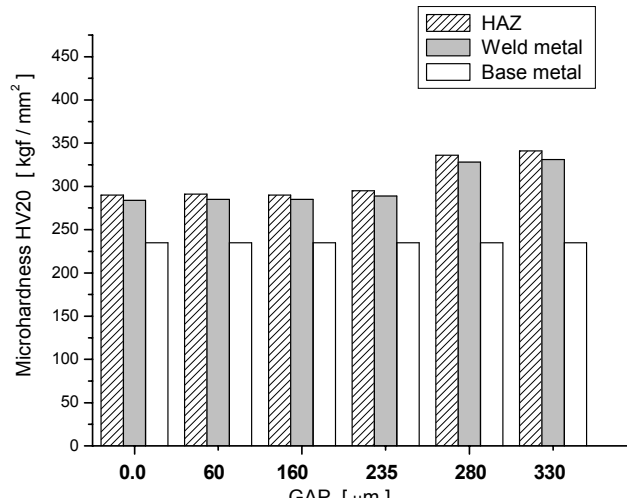
Figure 9. Hardness profile of base metal, HAZ and weld metal of AISI 304 steel as a function of the gap.

4. CONCLUSIONS

From the experimental results of the pulsed laser welding, the following conclusions may be drawn.

- Gap control is of considerable importance for weld quality in terms of fusion zone shape and profile.
- Joints with different gap have a pronounced effect on size and shape of the fusion zone. Presence of pores was observed in specimen with zero gap. Presence of spatters was observed in wider gaps
- Increase in the gap resulted in an increase in the top and bottom concavity, an decreased in the bead width and hence a decrease in the fusion zone transversal area.
- Fusion zone microstructure was insensitive to change in the gap. However, decrease in the fusion zone size resulted in a finer solidification structure due to high cooling rate.
- A dominant austenitic structure with no solidification cracking was obtained for all welds.
- Microhardness values in the fusion zone showed an increase with respect to those measured in the base metal. It has been related to the microstructural refinement induced by rapid cooling.

5. REFERENCES

American Welding Society, "Welding Processes", vol.2, 8th Ed., Miami, Fla., 1991.

American Welding Society, "Materials and Applications – part 2", vol.4, 8th Ed., Miami, Fla., 1998.

Delong W.T. Ferrite in austenitic stainless steel weld metal, Welding Journal, 1974, 53(7): 273s-286s.

Deng D.; Murakawa H. and Ueda Y.; Theoretical prediction of welding distortion considering positioning and gap between parts, International Journal of Offshore and polar Engineering, 2004, 14(2): 138-144.

Kawarito Y., Kito M. and Katayama S., In-process monitoring and adaptive control for gap in micro butt welding with pulsed YAG laser, Journal of Physics D: Applied Physics, 40 (2007), 183-190.

Lippold, J.C., Solidification behavior and cracking susceptibility of pulsed-laser welds in austenitic stainless steels, Welding Journal, 1994, 73(6):129s-139s.

Vitek, J.M., DasGupta, A. and David, S.A., Microstructural modification of austenitic stainless steels by rapid solidification, Metallurgical Transaction A, 14A, 1983,. 1833-1841.

Wouters M., Powell J. and Kaplan A., The influence of joint gap on the strength of hybrid Nd:yttrium-aluminum-garnet laser-metal inert gas welds, Journal of laser applications, 2006, 18(3): 181-184.

Zhou J. and Tsai H.L.; Porosity formation and prevention in pulsed welding, Journal of heat transfer-Transactions of the ASME, 2007, 129 (8): 1014-1024.

6. RESPONSIBILITY NOTICE

The authors are the only responsible for the printed material included in this paper.